

## Supplementary Materials

### 1. Methods

#### Multivariate Pattern Analysis

We used multivariate pattern analysis (MVPA) (Kriegeskorte et al., 2006) to examine brain regions in which spatial activation patterns could distinguish (1) auditory attention task from multisensory task, and (2) visual attention task from multisensory task.

Specifically, we used the searchlight approach combined with a hard-margin linear support-vector (SVM) machine classifier. The corresponding attention-related activation  $t$ -maps from SPM analysis were used as data input to the classifier. Then, we constructed a spherical neighborhood centered on each voxel in the brain with a radius of 6mm, and the data within that neighborhood was for classification. To estimate the performance of the classifier, we used a leave-one-subject-out cross-validation approach in which data from a subject is left out at a time as test set and data from the remaining subjects were used as training set to train the classifier. The class label estimated by the classifier on the test set was compared against the true class. The ratio of correctly estimated class labels to the total number of observations, hereafter referred to as cross-validation accuracy (CVA), was then computed. The resulting 3D map of CVA at every voxel was used to identify brain regions that distinguish between auditory task and multisensory task, as well as between visual task and multisensory task. Under the null hypothesis that there is no difference between the tasks, the CVAs were assumed to follow the binomial distribution  $B(N, p)$  with parameters  $N$  equal to the total number of observations and  $p$  equal to 0.5, assuming that under the null hypothesis, the probability of each task label is

equal. The CVAs were then converted to  $p$ -values using the binomial distribution. The significant multivariate patterns were determined using a voxel-wise height threshold of  $p\text{-val} < 0.01$  and an extent threshold of  $p\text{-val} < 0.01$  with family-wise error correction using a nonstationary suprathreshold cluster-size approach based on Monte-Carlo simulations (Nichols and Hayasaka, 2003), similar to the approach used for thresholding univariate activation patterns.

## 2. Figures and Tables

**Figure S1.** Reaction times for oddball stimuli in the auditory, visual, simultaneous multisensory and non-simultaneous multisensory tasks. Reaction time in the non-simultaneous multisensory task was significantly higher than all the other three tasks. ‘\*\*\*’:  $p < 0.01$ ; ‘\*\*\*’:  $p < 0.001$ . Sim-multisensory: simultaneous multisensory task in which auditory and visual stimuli were presented at the same time; NonSim-multisensory: non-simultaneous multisensory task in which auditory and visual stimuli were presented with a delay of 100ms.

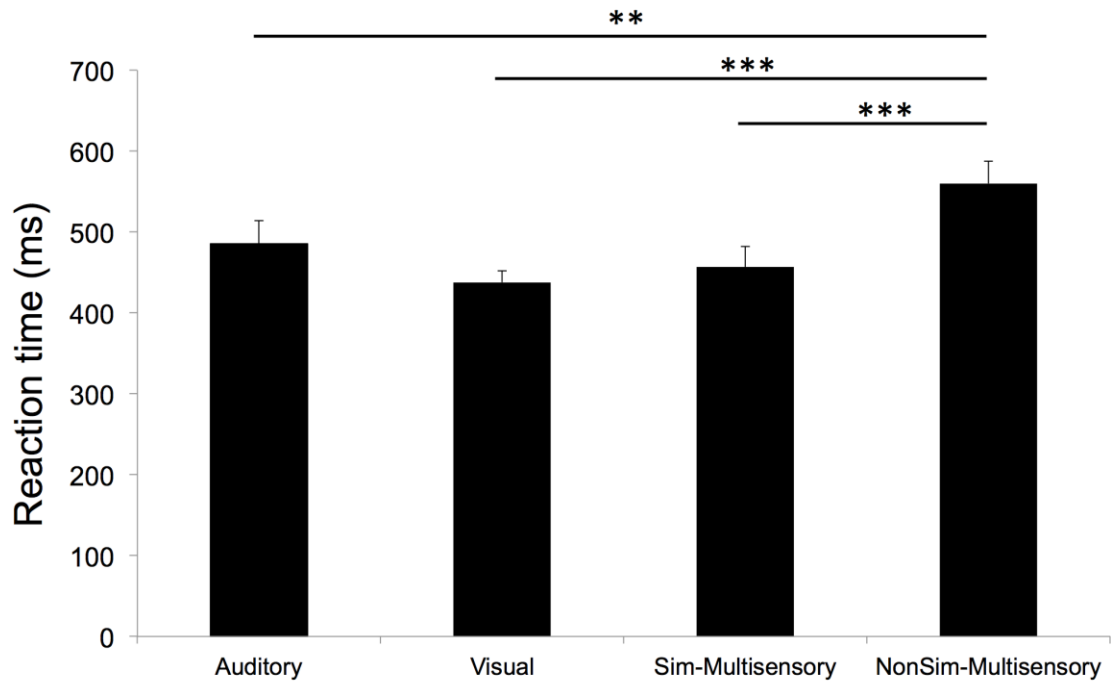


**Figure S2.** Attention-related brain activation patterns distinguishing multisensory and unisensory stimuli. Results of multivariate pattern analysis comparing (A) Multisensory auditory-visual vs. unisensory auditory deviants, and (B), Multisensory vs. unisensory visual deviants. rAI: right anterior insular cortex; dACC: dorsal anterior cingulate cortex.

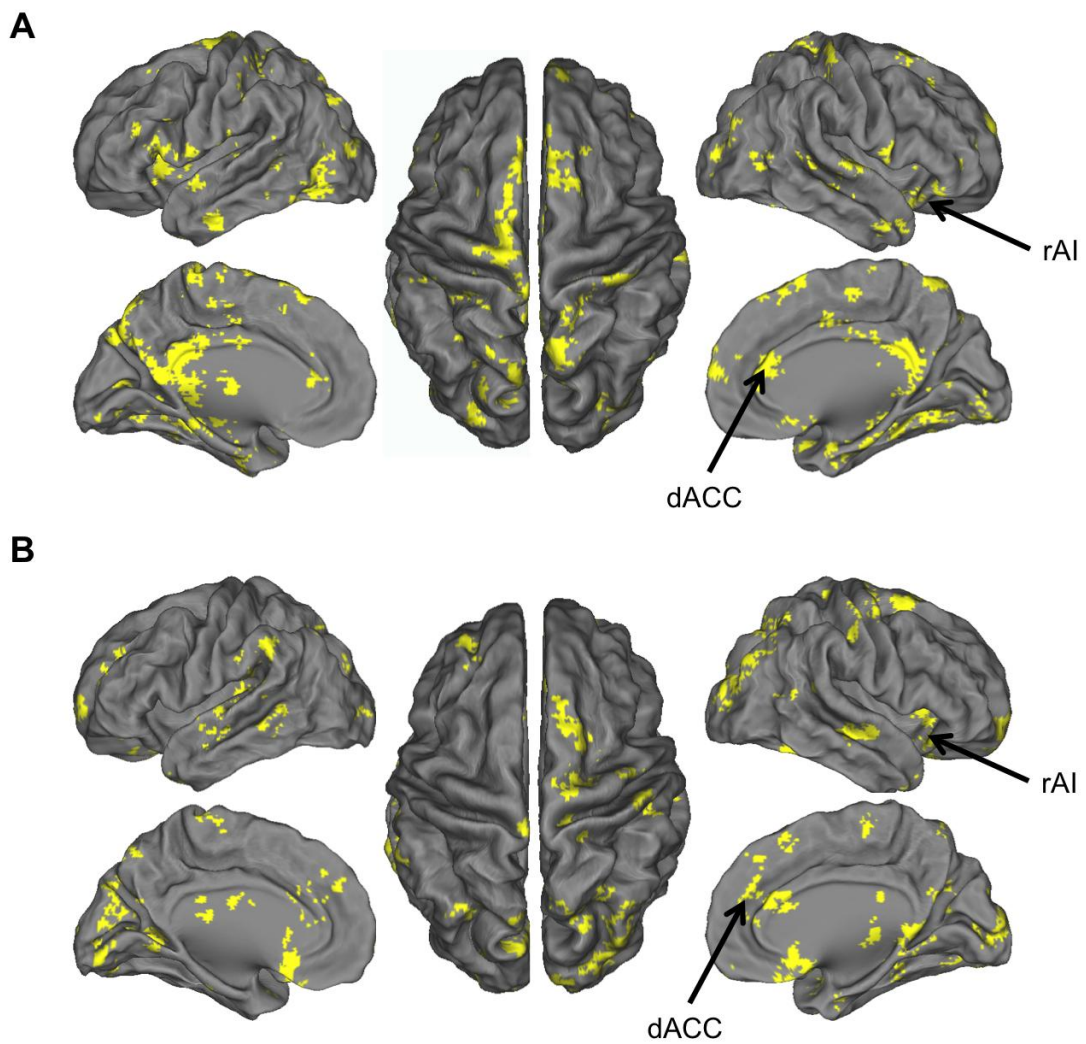


**Figure S3.** Attention-related dynamic causal interactions between the five nodes of neurocognitive networks in the left hemisphere. Significant causal interactions were observed between five key nodes in SN (blue) and CEN (green) in multisensory (A), auditory (B) and visual tasks (C). Across three tasks, the AI was the dominant source of casual influence. Results were shown with  $p < 0.01$  (Bonferroni corrected). D, Common causal interactions across the three attention tasks. E, Sum of unisensory causal interactions between the AI and dACC were significantly stronger than multisensory causal interactions. Results were shown with  $p < 0.01$  (Bonferroni corrected).

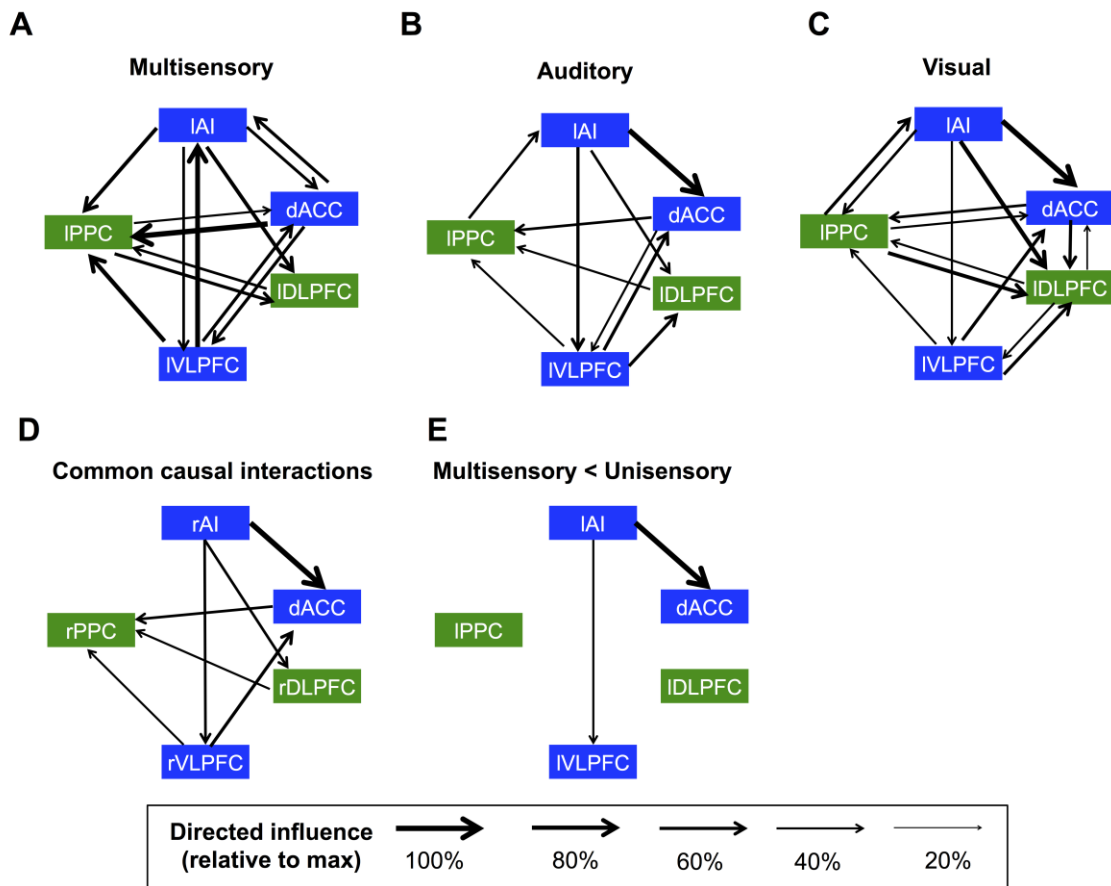


**Figure S4.** Causal outflow from regions in SN and CEN during multisensory attention task for nodes in the left hemisphere. IAI, dACC and IVLPFC all showed higher number of causal outflow connections (out degree) than IDLPFC. . ‘\*’:  $p < 0.05$ ; ‘\*\*’:  $p < 0.01$   
AI: anterior insular cortex; dACC: dorsal anterior cingulate cortex; DLPFC: dorsolateral prefrontal cortex; PPC: posterior parietal cortex; VLPFC: ventrolateral prefrontal cortex;  
l: left.

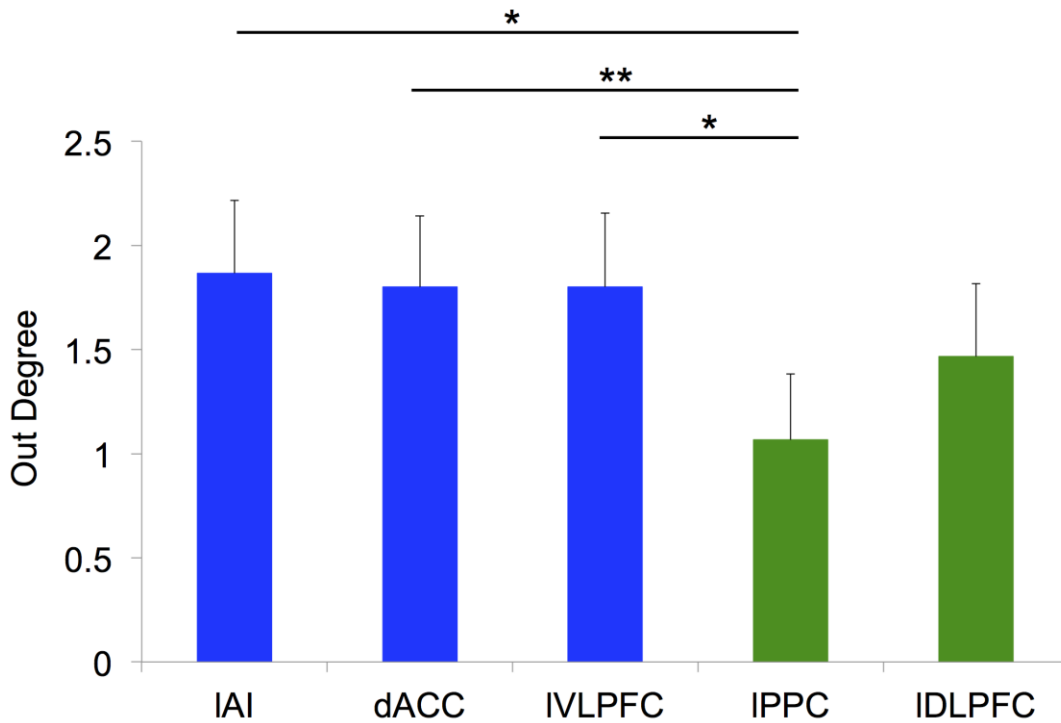


**Figure S5.** Attention-related dynamic causal interactions between the five nodes of the SN and CEN, and an additional STS node in the left hemisphere. Significant causal interactions were observed between six nodes in SN (blue), CEN (green) and STS (red) in multisensory (A), auditory (B) and visual tasks (C). Results were shown with  $p < 0.01$  (Bonferroni corrected). D, Common causal interactions across the three attention tasks. E, Sum of unisensory causal interactions between the AI and DLPFC, dACC and DLPFC, PPC and DLPFC were significantly stronger than multisensory causal interactions with  $p < 0.01$  (Bonferroni corrected). F, The same pattern was observed with  $p < 0.05$  (Bonferroni corrected). SN: Saliency Network; CEN: Central Executive Network; AI: anterior insular cortex; dACC: dorsal anterior cingulate cortex; DLPFC: dorsolateral prefrontal cortex; PPC: posterior parietal cortex; VLPFC: ventrolateral prefrontal cortex; STS: superior temporal sulcus; l: left.

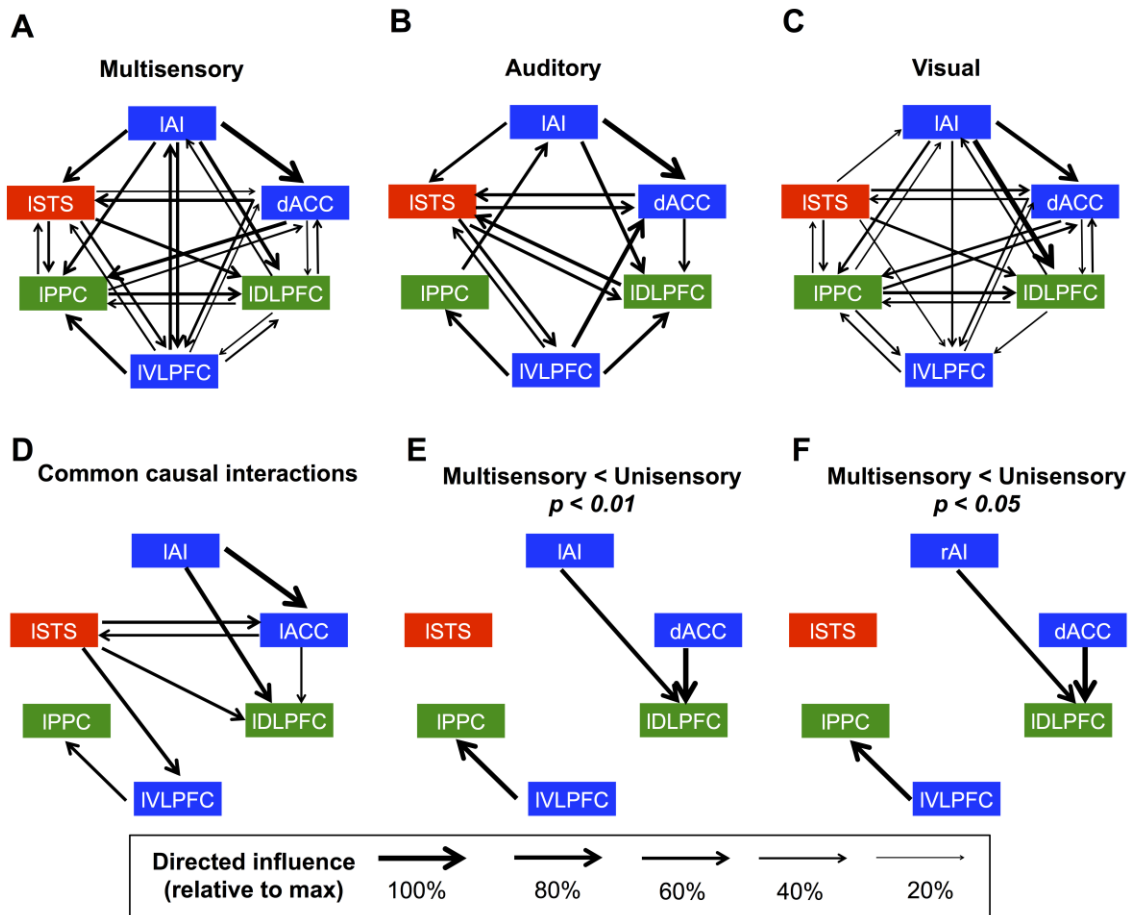


**Figure S6.** *Causal outflow during multisensory attention task.* Only lAI showed higher number of causal outflow connections (out degree) than IPPC. ‘\*’:  $p < 0.05$ . AI: anterior insular cortex; dACC: dorsal anterior cingulate cortex; DLPFC: dorsolateral prefrontal cortex; PPC: posterior parietal cortex; VLPFC: ventrolateral prefrontal cortex; STS: superior temporal sulcus; l: left;

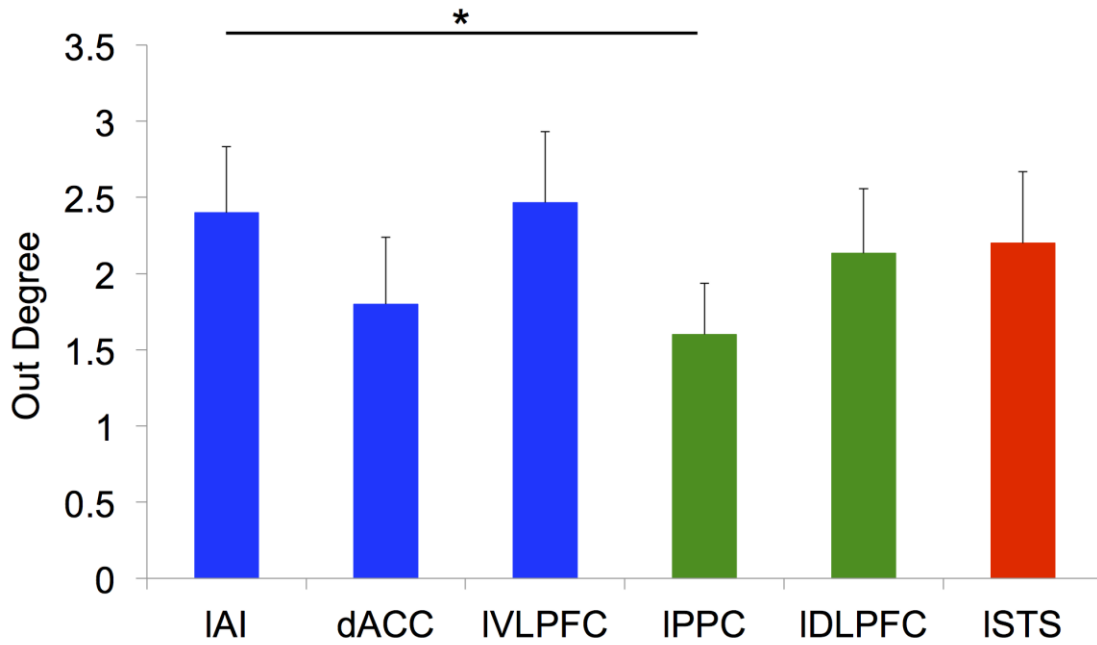




**Table S1.** Location of the left hemisphere SN and CEN nodes, and an additional node in the STS. SN: salience network; CEN: central executive network; AI: anterior insular cortex; dACC: dorsal anterior cingulate cortex; DLPFC: dorsolateral prefrontal cortex; PPC: posterior parietal cortex; VLPFC: ventrolateral prefrontal cortex; STS: superior temporal sulcus.

Region	Hemisphere	Brodmann Area	MNI coordinates (X, Y, Z)		
<b><i>SN</i></b>					
AI	Left	13	-34	20	-8
VLPFC	Left	46	-42	26	14
dACC		31	7	18	33
<b><i>CEN</i></b>					
DLPFC	Left	8	-46	20	44
PPC	Left	7	-40	-56	44
STS	Left	22	-51	-47	13

**Table S2.** Brain regions that showed significant responses to combined attention-related stimuli in the multisensory, auditory and visual attention tasks.

Region	Cluster Size	Peak F-statistic	MNI Coordinates		
			X	Y	Z
L cerebellum	1337	21.05	-26	-64	-26
L posterior parietal cortex	3134	19.67	-48	-34	56
L superior frontal gyrus	1282	15.45	-22	28	54
R cerebellum	1311	13.92	26	-66	-26
R posterior superior temporal gyrus	1608	11.95	60	-30	-2
L anterior insular cortex	454	11.45	-32	18	8
L precuneus	1001	11.35	-14	-62	16
R posterior parietal cortex	850	11.18	46	-32	44
L precentral gyrus	241	9.98	-60	8	2
R/R anterior cingulate cortex	444	9.85	-6	12	48
L lateral occipital cortex	1014	9.55	-38	-80	28
L frontal orbital cortex	171	8.92	-28	32	-18
L frontal pole	643	8.63	-12	66	28
R middle frontal gyrus	341	8.52	40	6	52
R lateral occipital cortex	840	8.07	48	-76	-8
L/R posterior cingulate gyrus	492	7.54	-6	-38	42
R anterior insular cortex	300	5.62	36	18	-2

## **Reference**

Kriegeskorte N, Goebel R, Bandettini P (2006) Information-based functional brain mapping. *Proceedings of the National Academy of Sciences of the United States of America* 103:3863-3868.

Nichols T, Hayasaka S (2003) Controlling the familywise error rate in functional neuroimaging: a comparative review. *Stat Methods Med Res* 12:419-446.